Asymmetric reversible diode-like resistive switching behaviors in ferroelectric $BaTiO_3$ thin films*

Zhang Fei(张 飞)[a], Lin Yuan-Bin(林远彬)[a], Wu Hao(吴 昊)[a], Miao Qing(苗 青)[a], Gong Ji-Jun(巩纪军)[a], Chen Ji-Pei(陈继培)[a], Wu Su-Juan(吴素娟)[a], Zeng Min(曾 敏)[a], Gao Xing-Sen(高兴森)[a]†, and Liu Jun-Ming(刘俊明)[b]‡

[a] *Institute for Advanced Materials, South China Normal University, Guangzhou* 510006, *China*
[b] *Laboratory of Solid State Microstructures, Nanjing University, Nanjing* 210093, *China*

(Received 26 March 2013; revised manuscript received 6 May 2013; published online 10 December 2013)

In this work, the resistive switching behaviors of ferroelectrictric $BaTiO_3/La_{0.67}Sr_{0.33}MnO_3$ heterostructures deposited by pulsed laser deposition are investigated. The $BaTiO_3$ films show both well-established *P*–*E* hysteresis loops, and asymmetric reversible diode-like resistive switching behaviors, involving no forming process. It is found that both the ON/OFF ratio and the stability of resistive switching are substantially dependent on operation voltage (V_{max}). At a V_{max} of 15 V, a large ON/OFF resistance ratio above 1000 is obtained at a V_{max} of 15 V, which is able to maintain stability up to 70-switching cycles. The above resistive switching behaviors can be understood by modulating interface Schottky barriers as demonstrated by *I*–*V* curve fitting.

Keywords: ferroelectrics, resistive switching, RRAM, pulsed laser deposition

PACS: 77.84.–s, 77.80.–e, 73.50.–h, 72.20.–i **DOI:** 10.1088/1674-1056/23/2/027702

1. Introduction

In the past decade, resistive random access memory (RRAM) devices have been the focus of intensively investigating a great variety of superior properties, such as nonvolatility, high speed, low energy, and high density, and considered as an ideal candidate for immerging nonvolatile memory.[1–7] The memory effect in RRAM relies on resistive switching material in which a resistance switching between high resistive (HRS) and low resistive state (LRS) can be reversibly triggered by applying an electric field. Recently, there has been an upsurge of research interest in ferroelectrically-related resistive switching effects.[7–10] In contrast to conventional chemically-related (e.g. redox) effects,[1–3] the variations of resistivity in ferroelectrics can be induced via the modulation of a ferroelectric conduction band by polarization reversal. This has the advantage of not being based on voltage-induced ion or defect migration, but on a purely electronic mechanism, which not only enables the fast and nondestructive read-out of the polarization states and enhances the stability and uniformity, but also avoids the undesirable forming process. Ferroelectric resistive switching behaviors in ultrathin ferroelectric films of $BaTiO_3$ (BTO),[9–14] Pb(Zr, Ti)O_3 (PZT),[15] and $BiFeO_3$(BFO)[16] have been widely studied, and are mainly attributed to the electronic quantum tunneling effects. In a recent study, large resistance variations exceeding two orders of magnitude, together with excellent retention of up to a few months and cycling endurance of more than 10^5 switching cycles, can be obtained in few nanometer-thick $BaTiO_3$ films.[12,13] More recently, a unique switchable diode effect was observed in thicker films or single crystalline ferroelectric $BiFeO_3$,[15–19] which has been explained by the polarization-dependent Schottky junction in ferroelectrics. By appropriately adjusting electrode-film interfaces or charge carrier concentrations, the resistive behaviors can be further tailored to have excellent stability and anti-fatigue properties, which is promising for applications in memory devices.[20,21]

However, there are still very few investigations into ferroelectric resistive switching in relatively thicker $BaTiO_3$ films, though the diode-like transport has been observed in its oxygen-deficient single crystal.[22] In this work, the resistive and ferroelectric behaviors in $BaTiO_3/La_{0.67}Sr_{0.33}MnO_3$ (BTO/LSMO) heterostructured thin films deposited by pulsed laser deposition (PLD) are examined. The BTO films show both well-established ferroelectric hysteresis loops, and unique forming free reversible diode-like resistive switching behaviors, which are related to the modulation of interface potential profile by polarization switching.

2. Experiment

The resistive device structure is schematically shown in Fig. 1(a), which consists of an LSMO bottom electrode on silicon substrate, a BTO active layer, and Au top electrodes. Here,

*Project supported by the National Natural Science Foundation of China (Grant Nos. 51072061, 51031004, and 51272078), the Program for Changjiang Scholars and Innovative Research Team in University, and the Priority Academic Program Development of Jiangsu Higher Education Institutions, China.

†Corresponding author. E-mail: xingsengao@scnu.edu.cn
‡Corresponding author. E-mail: liujm@nju.edu.cn

© 2014 Chinese Physical Society and IOP Publishing Ltd

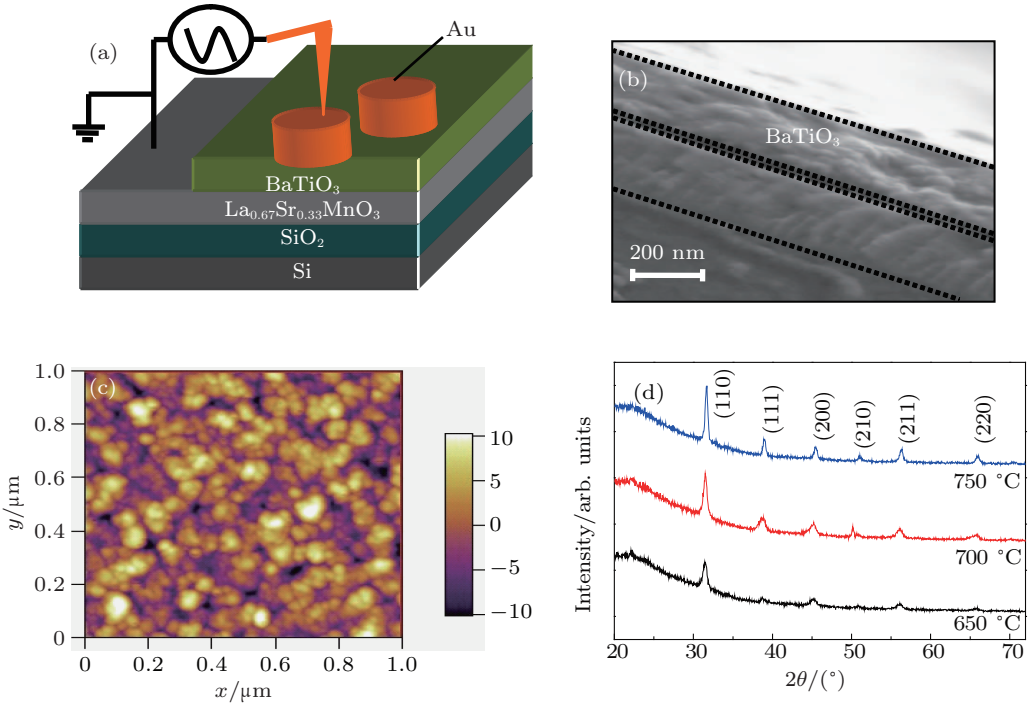


Fig. 1. (color online) (a) Schematic diagram for the resistive switching cells consisting of BTO-based multilayer capacitor structures; (b) SEM cross-section image for the BTO heterostructure deposited at 700 °C on LSMO/SiO_2/Si substrate; (c) AFM surface topographic micrograph for the as-deposited BTO film; and (d) X-ray diffraction patterns for BTO thin films deposited at three different temperatures.

the LSMO bottom layers and the BTO films were sequentially deposited on SiO_2/Si substrates by pulsed laser deposition using a KrF excimer laser with a wavelength of 248 nm. Both LSMO layers and BTO layers were deposited at various ambient temperatures (from 650 °C to 750 °C) using the same deposition parameters (e.g. pulse energy = 1.99 J/cm^2 and repetition = 5 Hz). For electrical measurements, Au top electrodes with 140 μm in diameter were deposited on the top of BTO film through a shadow mask using a dc sputtering coater. The thickness of the LSMO layer is ∼ 30 nm, and that of the BTO film is ∼ 300 nm, both of which were determined by a scanning electron microscope (SEM) cross-sectional image (Fig. 1(b)).

The surface topography for the BTO film deposited at 700 °C was monitored by atomic force microscopy (AFM, Asylum Research, Cypher), which clearly shows spherical grains of ∼ 40 nm in diameter and an average roughness of ∼ 3.95 nm (Fig. 1(c)). The crystallization features of BTO films deposited at three different ambient temperatures were confirmed by X-ray diffraction (X'Pert PRO, PANalytical) using the thin film diffraction mode in order to suppress the diffraction signals from both substrate and bottom electrode layer. As shown in Fig. 1(d), all the diffraction peaks from the films can be indexed by various BTO planes without a detectable impurity phase. The current–voltage (I–V) characteristics were measured by a Keithley 6430 low resistive source meter at room temperature, using a staircase voltage in steps of 0.1 V and a duration delay of 0.1 s/step. As the delay time for each step is considerably longer than that of fast transient current from polarization switching, the I–V curve should exhibit a quasi-static behavior. The ferroelectric hysteresis loops were obtained using a Precision Materials Analyzer (Multiferroic, Radiant) at a frequency of 1 kHz.

3. Results and discussion

Figure 2(a) shows the room temperature ferroelectric hysteresis loops for the BTO thin films deposited at 700 °C, in which well-established hysteresis loops can be observed. The remnant polarization (P_r) for the BTO film increases gradually with the rising of operation bias voltage (V_{max}). The remnant polarization (P_r) for the BTO film is measured to be ∼ 8.5 μC/cm^2 at V_{max} of 15 V. Although this value is smaller than that of perfectly strained epitaxial BTO films,[23] it is still considerably large compared with those reported values for polycrystalline BTO films or unstrained epitaxial BTO films,[24,25] wherein only slim hysteresis loops can be obtained, owing to their severe depolarizations.

The resistive switching properties at various values of operation bias voltage (V_{max}) for the BTO film deposited at 700 °C are illustrated in Fig. 2(b). All the I–V curves show apparent asymmetric current rectification behaviors, as well as well-recognized resistive switching loops in a positive bias voltage range. To further reveal the low current I–V behavior, a semi-logarithmic I–V curve at a V_{max} of 18 V was plotted in Fig. 2(c). It is found that resistive switching characteristics can be well identified in both positive and negative bias ranges, although the variation of resistance in a negative bias

range is much smaller than that at positive bias, which is likely to be due to the significant current rectification. More interestingly, unlike the typical bipolar resistive switching, which shows the remaining HRS–HRS (or LRS–LRS) when applied bias sweeps forwards (or backwards) through the zero voltage point, the resistive states in our BTO film show apparent HRS–LRS (or HRS–LRS) as the bias crosses the zero voltage, showing a characteristic of so-called switchable diode effect. To further verify this, we measured the *I*–*V* curves after poling by different voltages (±18 V) in the voltage range as shown in the inset of Fig. 2(c). Both *I*–*V* curves exhibit typical characteristics of diode effect. The up state (+18 V, HRS) displays a forward diode-like behavior, whereas the down state (–18 V, LRS) exhibits a backward diode effect, further confirming the switchable diode-like resistive switching behaviors. A similar phenomenon (though not so asymmetric) has been previously reported in BFO thin film[19,20] and single crystal BFO and BTO,[17,22] which has been considered as an important feature for ferroelectrically-related resistive switching.

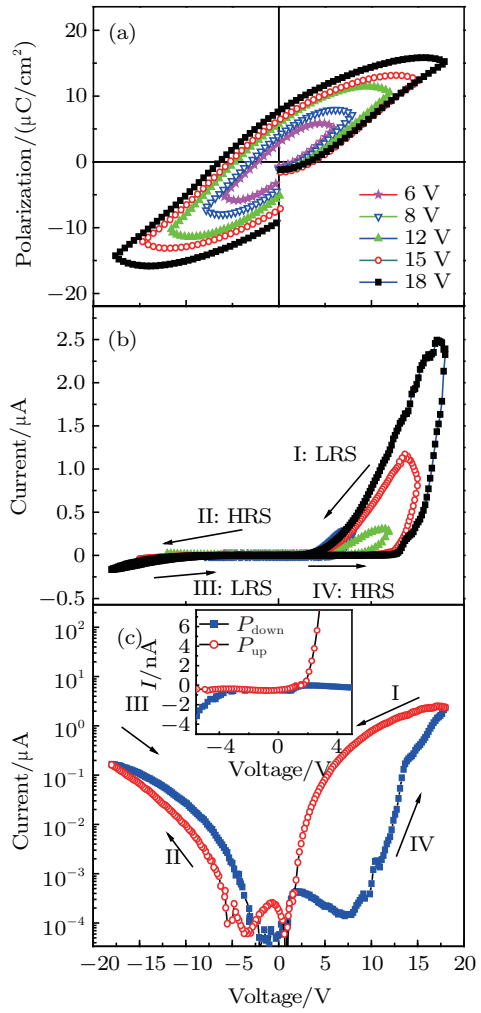


Fig. 2. (color online) (a) *P*–*V* hysteresis loops and (b) *I*–*V* hysteresis curves at different values of operation bias voltage (V_{max}) for the BTO film deposited at 700 °C, (c) semi-logarithmic plot of an *I*–*V* hysteresis loop at V_{max} 18 V. The inset shows the low field *I*–*V* curves for two different polarization states.

It is worth mentioning that our BTO films are rather robust and able to withstand dc voltages as high as 20 V, thus enabling the further exploration of high field *I*–*V* characteristics. The maximum ON/OFF resistance ratios are extracted at certain voltages where the largest resistance ratio can be found (e.g. at V_{max} of 18 V, V_{read} of 7 V). The ON/OFF ratio is greatly dependent on V_{max}, which increases quickly from 688 at V_{max} of 8 V to 2601 at 18 V, which also implies that it is a multilevel resistive switching. It is noted that the dependence of ON/OFF resistance ratio is apparently correlated with the remnant polarization, which is also greatly dependent on the maximum applied voltage. The large resistance variation is larger than that of BFO film and that induced by the BTO-based ferroelectric tunneling effect, which is desirable for memory applications.[12,19] The operation voltages in our BTO are a little too large for real application, nevertheless the operation voltages can further be reduced to meet certain applications by properly adjusting the film thickness or deposition parameters. It is also noted that resistive switching phenomena have also previously been reported in BTO films,[26,27] but these films were too leaky too show good ferroelectric hysteresis loops, and their resistive switching properties are dominated by defect related mechanisms.

To further examine the stability of the resistive switching, the *I*–*V* testing was repeated for about 70-cycles. Figure 3 shows the *I*–*V* hysteresis loops versus repeating cycle. At small bias voltages (e.g. 6 V or 8 V), the resistive switching is not very stable against repetition cycle, in which the ON/OFF resistance ratio drops down fast with the elongating of switching cycle. In comparison, at higher bias voltages (above 12 V), the resistances become very stable. As shown in the inset of Fig. 3(d), the BTO film at V_{max} of 15 V demonstrates a stable ON/OFF resistance ratio of 1024 without apparent fluctuation up to 70-cycles. The reason for the different stabilities is still not clear. It is likely to be due to the fact that the interface potential profiles are not very stable after applying a low voltage bias, while for a high voltage bias, rather stable interface potential variation can be induced, consequently leading to the enhanced repeatability against the switching cycle. As the resistive switching is closely related to the polarization status, at low operation voltages (e.g. 6 V, 8 V), the polarization state is not saturated, containing lots of movable domain walls and charge trapping sides, which are rather unstable against repeated switching cycles. At high operation voltages (e.g. 12 V, 15 V), the polarization states become more or less saturated, and the unstable domain wall or charge trapping sites have greatly reduced, contributing to the repeatable resistive switching behaviors.

In metal oxides, the conductive mechanisms are rather complicated, as defect mediated transport effects, such as grain boundary, ionic or electrochemical effects,[4,6] may also lead to *I*–*V* hysteresis. To further clarify the origin of the

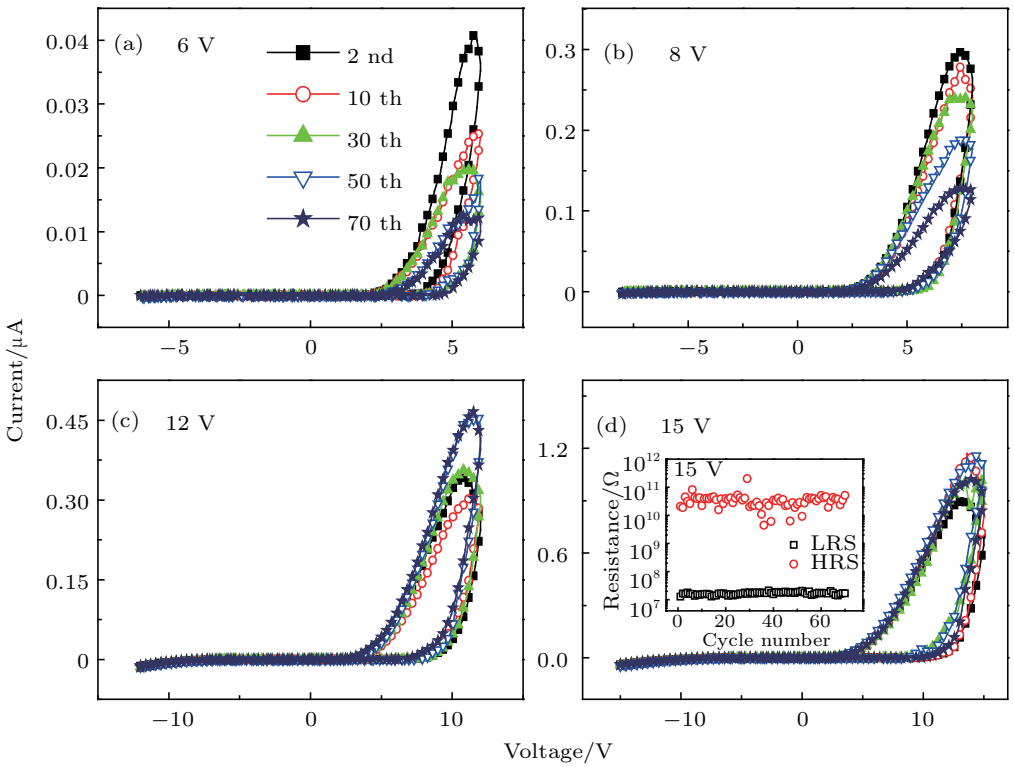


Fig. 3. (color online) Curves of *I*–*V* versus resistive switching cycle for the BTO film deposited at 700 °C at different bias voltages: (a) 6 V, (b) 8 V, (c) 12 V, and (d) 15 V. The inset in panel (d) shows HRS and LRS resistant values against 70 switching cycles at a V_{max} of 15 V.

switching behaviors, we examine the conductive mechanisms for the four individual states. It is found that the *I*–*V* curves can be well fitted by the Schottky equation,[28–30]

$$J = A^{**}T^2 \exp\left[\frac{\Phi - (e^3/4\pi\varepsilon_0 d\varepsilon_r)^{1/2}V^{1/2}}{kT}\right], \qquad (1)$$

where A^{**} is the Richardson constant, T the temperature (which is set at 295 K), Φ the barrier potential arising from the different work functions between the metal electrodes and oxide insulator, e the electronic charge, ε_0 the permittivity of free space, d the film thickness, ε_r the optical dielectric constant, V the applied voltage, and k Boltzmann constant. As shown in Fig. 4(a), *I*–*V* curves for the four different states can be fit by the same equation under the assumption of $A^{**} = 1 \times 10^6$ A·m^{-2}·K^{-2} and $T = 295$ K.[31] By fitting, we are able to extract the four different Schottky barriers for both film–electrode interfaces at different states, and construct a schematical diagram for the interface Schottky barriers based on the extracted Schottky barriers as indicated in Fig. 4(b). It is found that at the LSMO/BTO interface, the Schottky barrier is rather high (1.36 eV) at LRS while it becomes much lower (0.63 eV) at HRS. From the literature,[28] the work function of LSMO is around 4.8 eV, and the electron affinity of oxide is around 3.6 eV, which leads to a Schottky barrier of 1.2 eV (the difference between metal work function and oxide electron affinity) for BTO/LSMO interface without considering the modulation of interface potential barriers. It is also interesting to see that there exists a relatively large potential variation ($\Delta\Phi = 0.61$ eV) in Schottky barrier height between

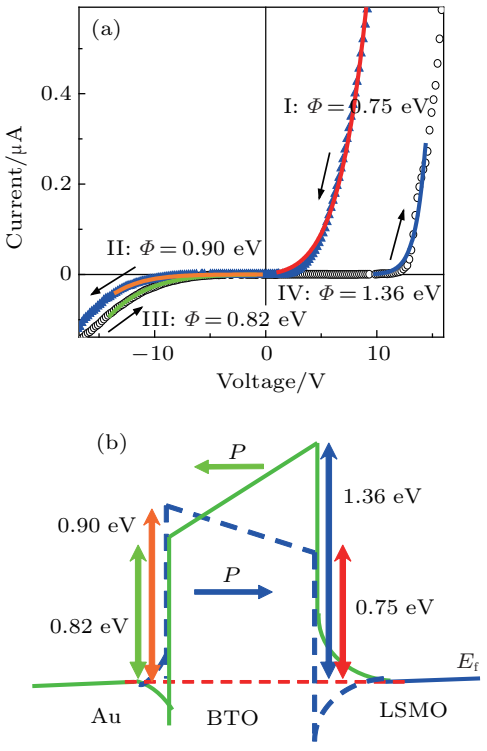


Fig. 4. (color online) (a) Typical *I*–*V* curves for the BTO film measured at 18 V, which is fitted by the Schottky emission equation, from which four different Schottky barriers can be extracted; (b) schematic diagram of potential profiles for the BTO-electrode interfaces based on the above fitting, which illustrates the changes in Schottky barrier.

in the HRS and LRS at BTO/LSMO interfaces, corresponding to different potential barriers: 0.75 eV at LRS and 1.36 eV at HRS, whereas for the BTO/Au interface, a much smaller potential barrier difference ($\Delta\Phi = 0.08$ eV) is observed at the BTO/Au interface. These can explain the large ON/OFF resistance ratio for the two resistive states in the positive bias voltage range and the smaller resistance difference in the negative bias range well.

The direct evidence for the variation in Schottky barriers has been reported in oxide films recently,[32–34] but the origin of the variation ($\Delta\Phi$) is still controversial. There are some possible explanations, including the migration of oxygen vacancies,[35–37] incomplete screening of ferroelectric polarization charge by metal electrodes,[38] and charge trapping and detrapping process.[32,39] In our case, the observed modulation in interface Schottky barrier is very similar to previous experimental and theoretical reports on switchable diode-like resistive switching behaviors in ferroelectric $BiFeO_3$ single crystal and thin film as well as in Pb(Zr, Ti)O_3 film, which can be well explained by the ferroelectrically-related incomplete screening of polarization charge scenario.[17,19–21] From our fitting, the BTO/LSMO interface has a larger $\Delta\Phi$ on polarization reversal due to its longer screening length, whereas the Au/BTO interface possesses a shorter screening length corresponding to the smaller $\Delta\Phi$, which is in good agreement with this scenario. Besides this, other extrinsic effects, e.g. oxygen vacancies[32,40] and moisture, may also affect the interface potential barrier. Further studies are still needed to accurately ascertain the respective contributions for the above resistive switching behaviors.

4. Conclusions

The ferroelectric and resistive switching properties in BTO/LSMO heterostructrued films are carefully examined. It is found that the heterostructured films exhibit both well-established ferroelectric hysteresis loop and switchable diode like forming free resistive switching behavior, along with apparent current rectification behaviors. By properly adjusting the testing parameter, a large and stable resistance ON/Off ratio above three orders in magnitude can be obtained, exhibiting promising properties for RRAM application. The observed *I–V* curves can be well-fitted by a Schottky emission equation, revealing an apparent variation in Schottky barriers in response to polarization switching, which can account for the above resistive switching behavior.

References

[1] Waser R and Aono M 2007 *Nat. Mater.* **6** 833
[2] Shibuya K, Dittmann R, Mi S and Waser R 2010 *Adv. Mater.* **22** 411
[3] Meijer G I 2008 *Science* **319** 1625
[4] Jeong D S, Thomas R, Katiyar R S, Scott J F, Kohlstedt H, Petraru A and Hwang C S 2012 *Rep. Prog. Phys.* **75** 076502
[5] Liu S, Li Y T, Wang Y, Long S B, Lü H B, Liu Q, Wang Q, Zhang S, Lian W T and Liu M 2011 *Chin. Phys. B* **20** 017305
[6] Sawa A 2008 *Mater. Today* **11** 28
[7] Yang J J, Strukov D B and Stewart D R 2013 *Nat. Nanotechnol.* **8** 13
[8] Velev J P, Duan C G, Belashchenko K D, Jaswal S S and Tsymbal E Y 2007 *Phys. Rev. Lett.* **98** 137201
[9] Kohlstedt H, Petraru A, Szot K, Rüdiger A, Meuffels P, Haselier H, Waser R and Nagarajan V 2008 *Appl. Phys. Lett.* **92** 062907
[10] Garcia V, Fusil S, Bouzehouane K, Enouz-Vedrenne S, Mathur N D, Barthelemy A and Bibes M 2009 *Nature* **460** 81
[11] Gao X S, Liu J M, Au K, and Dai J Y 2012 *Appl. Phys. Lett.* **101** 142905
[12] Chanthbouala A, Garcia V, Cherifi R O, Bouzehouane K, Fusil S, Moya X, Xavier S, Yamada H, Deranlot C, Mathur N D, Bibes M, Barthélémy A and Grollier J 2012 *Nat. Mater.* **11** 860
[13] Chanthbouala A, Crassous A, Garcia V, Bouzehouane K, Fusil S, Moya X, Allibe J, Dlubak B, Grollier J, Xavier S, Deranlot C, Moshar A, Proksch R, Mathur N D, Bibes M and Barthélémy A 2012 *Nat. Nanotechnol.* **7** 101
[14] Kim D J, Lu H, Ryu S, Bark C W, Eom C B, Tsymbal E Y and Gruverman A 2012 *Nano Lett.* **12** 5697
[15] Pantel D, Lu H D, Goetze S, Werner P, Kim D J, Gruverman A, Hesse D and Alexe M 2012 *Appl. Phys. Lett.* **100** 232902
[16] Bea H, Bibes M, Cherifi S, Nolting F, Warot-Fonrose B, Fusil S, Herranz G, Deranlot C, Jacquet E, Bouzehouane K and Barthelemy A 2006 *Appl. Phys. Lett.* **89** 242114
[17] Choi T, Lee S, Choi Y J, Kiryukhin V and Cheong S W 2009 *Science* **324** 63
[18] Yang C H, Seidel J, Kim S Y, Rossen P B, Yu P, Gajek M, Chu Y H, Martin W, Holcomb M B, He Q, Maksymovych P, Balke N, Kalinin S V, Baddorf A P, Basu S R, Scullin M L and Ramesh R 2009 *Nat. Mater.* **8** 485
[19] Wang C, Jin K J, Xu Z T, Wang L, Ge C, Lu H B, Guo H Z, He M and Yang G Z 2011 *Appl. Phys. Lett.* **98** 192901
[20] Jiang A Q, Wang C, Jin K, Liu X B, Scott J F, Hwang C S, Tang T A, Lu H B and Yang G Z 2011 *Adv. Mater.* **23** 1277
[21] Hu Z Q, Li Q, Li M Y, Wang Q W, Zhu Y D, Liu X L, Zhao X Z, Liu Y and Dong S X 2013 *Appl. Phys. Lett.* **102** 102901
[22] Won C J, Park Y A, Lee K D, Ryu H Y and Hur N 2011 *J. Appl. Phys.* **109** 084108
[23] Choi K J, Biegalski M, Li Y L, Sharan A, Schubert J, Uecker R, Reiche P, Chen Y B, Pan X Q, Gopalan V, Chen L Q, Schlom D G and Eom C B 2004 *Science* **306** 1005
[24] Kuwabara M, Takahashi S and Kuroda T 1993 *Appl. Phys. Lett.* **62** 3372
[25] Ding B F and Zhou S Q 2011 *Chin. Phys. B* **20** 127701
[26] Yan Z B, Guo Y Y, Zhang G Q and Liu J M 2011 *Adv. Mater.* **23** 1351
[27] Zhang T J, Pan R K, Ma Z J, Duan M G, Wang D F and He M 2011 *Appl. Phys. Lett.* **99** 182106
[28] Scott J F 2000 *Ferroelectric Memories* (Berlin: Springer)
[29] Sze S M 1981 *Physics of Semiconductor Devices* (New York: Wiley)
[30] Lampert M A and Mark P 1970 *Current Injection in Solids* (New York: Academic Press)
[31] Pantel D and Alexe M 2010 *Phys. Rev. B* **82** 134105
[32] Zou X, Ong H G, You L, Chen W G, Ding H, Funakubo H, Chen L and Wang J L 2012 *AIP Advances* **2** 032166
[33] Huang B C, Chen Y T, Chiu Y P, Huang Y C, Yang J C, Chen Y C and Chu Y H 2012 *Appl. Phys. Lett.* **100** 122903
[34] Wu C L, Lee P W, Chen Y C, Chang L Y, Chen C H , Liang C W, Yu P, He Q, Ramesh R and Chu Y H 2011 *Phys. Rev. B* **83** 020103
[35] Rozenberg M J, Inoue I H and Sanchez M J 2004 *Phys. Rev. Lett.* **92** 178302
[36] Gao P, Wang Z, Fu W, Liao Z, Liu K, Wang W, Bai X and Wang E 2010 *Micron* **41** 301
[37] Hur J H, Lee M J, Lee C B, Kim Y B and Ki C J 2010 *Phys. Rev. B* **82** 155321
[38] Watanabe Y 1999 *Phys. Rev. B* **59** 257
[39] Wu W, Guest J R, Horibe Y, Park S, Choi T, Cheong S W and Bode M 2010 *Phys. Rev. Lett.* **104** 217601
[40] Buzio R, Gerbi A, Gadaleta A, Anghinolfi L, Bisio F, Bellingeri E, Siri A S and Marre D 2012 *Appl. Phys. Lett.* **101** 243505